

## Supporting Information

# Homotropic and Heterotropic Allosteric Regulation of Supramolecular Chirality

Mohit Kumar and Subi J. George\*

*Supramolecular Chemistry Laboratory, New Chemistry Unit,  
Jawaharlal Nehru Centre for Advanced Scientific Research (JNCASR), Bangalore,  
India-560064. E-mail: [george@jncasr.ac.in](mailto:george@jncasr.ac.in); Fax: +91 80 22082760; Tel: +91 80 22082964*

## Table of Contents

1. General Methods
2. Synthesis
3. Supporting Figures

### 1. General Methods

**Transmission Electron Microscopy (TEM):** TEM measurements were performed on a JEOL, JEM 3010 operated at 300 kV. Samples were prepared by placing a drop of the solution on carbon coated copper grids followed by drying at room temperature. The images were recorded with an operating voltage 300 kV. In order to get a better contrast sample was stained with uranyl acetate (1 wt % in water) before the measurements. For TEM, water was used instead of aq. HEPES solution to avoid masking of nanostructures due to HEPES deposition upon drying.

**Optical Measurements:** Electronic absorption spectra were recorded on a Perkin Elmer Lambda 900 UV-Vis-NIR Spectrometer and emission spectra were recorded on Perkin Elmer Ls 55 Luminescence Spectrometer. UV-Vis and emission spectra were recorded in 10 mm path length cuvettes. Fluorescence spectra of solutions were recorded with 470 nm and 570 nm excitation wavelength as per the requirement. Circular Dichroism measurements were performed on a Jasco J-815 spectrometer where the sensitivity, time constant and scan rate were chosen appropriately. Corresponding temperature dependent measurements were performed with a CDF – 426S/15 Peltier-type temperature controller with a temperature range of 263-383 K and adjustable temperature slope.

**Sample Preparation:** All samples for spectroscopic measurements were prepared by injecting the stock solution of **PDPA** (solvent MeCN) into required volume of solvent (aq. HEPES buffer in

MeCN, wherever applicable). To that required amount of phosphates were injected and the solution was mixed by manual shaking before measurements.

Aq. HEPES buffer was prepared by making 10 mM solution of the compound in water.

Phosphates stock solutions were prepared in  $10^{-2}$  M concentration by dissolving the required amount of compound in HEPES buffer solution.

**Materials:** All chemicals / solvents were purchased from the commercial sources and were used as such. Spectroscopic grade solvents were used for all optical measurements.

Legends in graphs represent molar equivalents with respect to **PDPA**.

## 2. Synthesis

PDPA was synthesized and characterized according to the literature procedure.<sup>S1</sup>

## 3. Supporting Figures

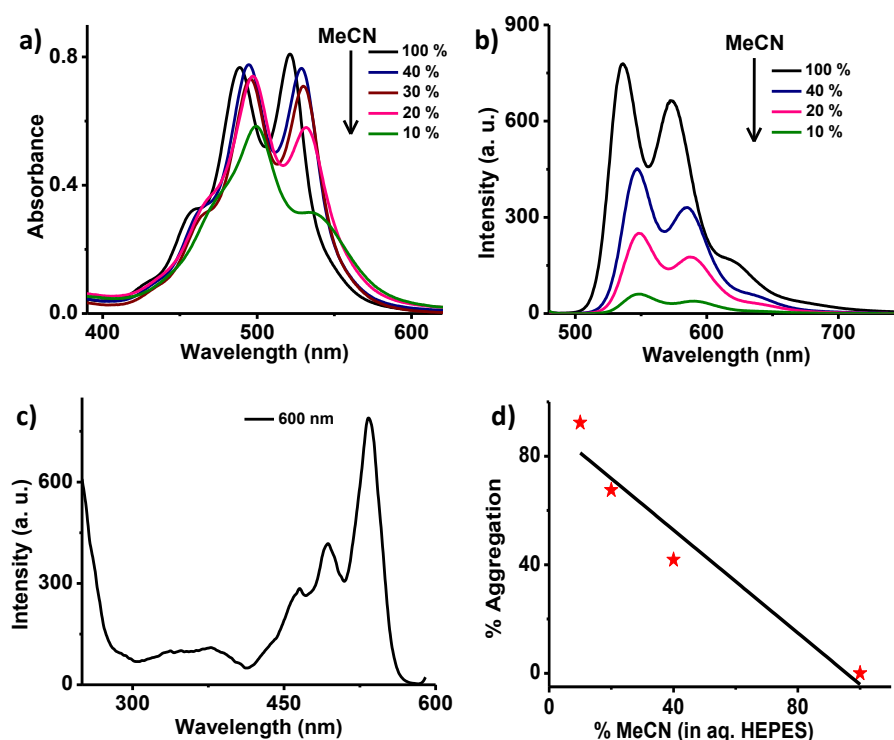


**Fig. S1** Self-assembly of PDPA: Solvent dependent a) absorption and b) emission spectra ( $\lambda_{exc}=470$  nm) of **PDPA** with varying percentages of MeCN in aq. HEPES buffer ( $c = 2 \times 10^{-5}$  M). c) Excitation spectra of **PDPA** assembly collected at 600 nm showing monomeric features (10 % MeCN in aq. HEPES solution,  $c = 2 \times 10^{-5}$  M). d) Plot of percentage aggregation at varying composition of MeCN in HEPES. This was obtained from the emission quenching data shown in b), where emission of MeCN solution was taken as 100 % monomers and completely aggregated emission to be non-emitting (zero in intensity).

The UV/Vis absorption spectrum of **PDPA** in MeCN showed sharp vibronic features of electronic transition at 460 nm, 488 nm and 521 nm, characteristic of monomeric PBI chromophores (Figure S1 a) (The intensity ratio of the two most intense band was 0.94, which is high compared to known PBI monomers, indicating

the existence of weak interchromophoric interactions even in MeCN at this concentration). Upon increasing percentages of aq. HEPES buffer in MeCN, broadening of absorption spectra and change of relative absorbance peak ratio was observed. Fluorescence signal ( $\lambda_{\text{ex}} = 470 \text{ nm}$ ) in b) showed sharp bands at 536 nm, 572 nm and 625 nm in MeCN which are characteristics of monomer emission of PBI. Upon increasing composition of aq. HEPES, we see a gradual quenching of the monomer emission with no additional band. Also the excitation spectra collected at 600 nm revealed its monomeric origin. These are signatures of typical non fluorescent H-type aggregates in PBI systems.

Plot of % aggregation in d) show that at 10 % MeCN in aq. HEPES buffer,  $\sim 93\%$  of **PDPA** molecules are aggregated. Thus the shape of CD titration shown in Fig. 2d of main text cannot be due to low degree of aggregation.

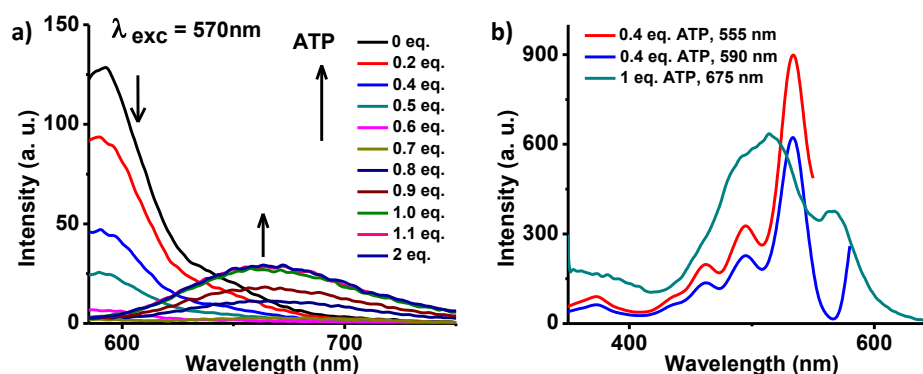


**Fig. S2** Emission and excitation spectral changes upon H1 to H2 transition of PDPA assembly, induced by ATP: a) Emission spectra upon selective excitation of aggregate at  $\lambda_{\text{exc}} = 570 \text{ nm}$ . b) Comparative excitation spectra at various states of aggregation i.e. in **H1** and **H2** state collected at various fluorescence bands. All measurements were done in 10 % MeCN in aq. HEPES solution,  $c = 2 \times 10^{-5} \text{ M PDPA}$ .

These experiments clearly show the mutually exclusive nature of the **H1** and **H2** states.

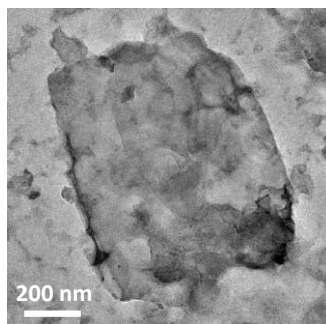


**Fig. S3** TEM image of nanosheets obtained from  $2 \times 10^{-5} \text{ M}$  solution of **PDPA** (10 % MeCN in water).

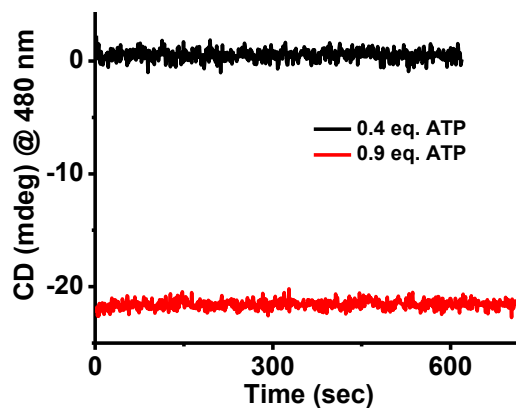


**Fig. S4** Time dependent variation in CD signal with addition of 0.4 eq. and 0.9 eq. of ATP (10 % MeCN in aq. HEPES solution,  $c = 2 \times 10^{-5}$  M PDPA). This data show that the phosphate binding and its supramolecular organization at H1 and H2 state do not show any kinetic effects.

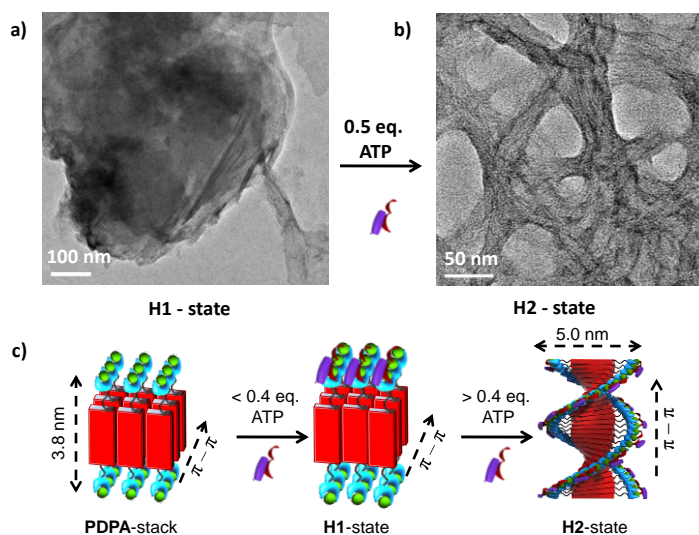


**Fig. S5** Additional TEM images of a) **H1** (0.4 eq. ATP) and b) **H2** (0.9 eq. ATP) states of **PDPA**-assembly showing the morphology transition from 2-D sheets to 1-D nanofibers (10 % MeCN in water,  $c = 2 \times 10^{-5}$  M), upon ATP binding. c) Schematic depicting the morphology transition of PDPA-assembly upon ATP binding along with the probable molecular organization in each states.

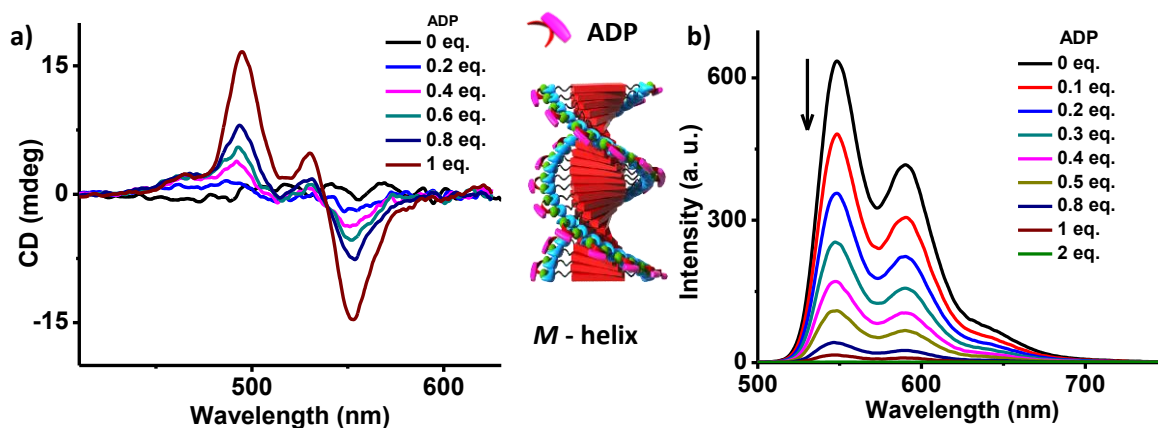


**Fig. S6** Binding of ADP to PDPA-assembly: Variation in a) CD spectra b) emission spectra of **PDPA** upon titration with ADP (10 % MeCN in aq. HEPES solution,  $c = 2 \times 10^{-5}$  M). In the middle is the schematic representation of ADP bound helical stacks which is opposite in handedness w.r.t ATP bound stacks. Legends in the graph represent molar equivalents with respect to **PDPA**.

Binding to adenosine diphosphate (ADP) also produced a negative bisignated CD signal, negative at higher wavelength (557 nm) followed by positive at 496 nm, an opposite bisignated spectra when compared to ATP bound stacks. Unlike ATP binding, ADP did not show any allosteric effect indicating a different mode of binding in these cases. Even the emission spectra changes on ADP binding showed just quenching of monomer emission without evolution of any additional band, confirming formation of **H1** aggregates.

At this point we don't really understand the exact reason for the reversal of CD signal obtained with ATP and ADP. We are investigating it in details with the help of MD simulations.

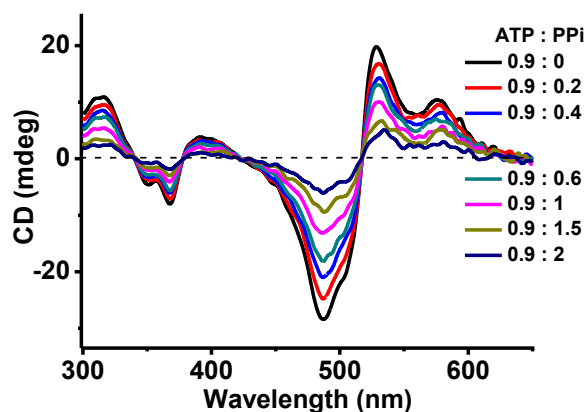


**Fig. S7** Decrease in CD signal of the **H2**-state of the **PDPA**-assembly upon competitive replacement of ATP by PPI. (10 % MeCN in aq. HEPES solution,  $c = 2 \times 10^{-5}$  M).

This explains the Figure 4a in the main text, which shows a decrease in CD signal intensity at higher equivalents of PPI.

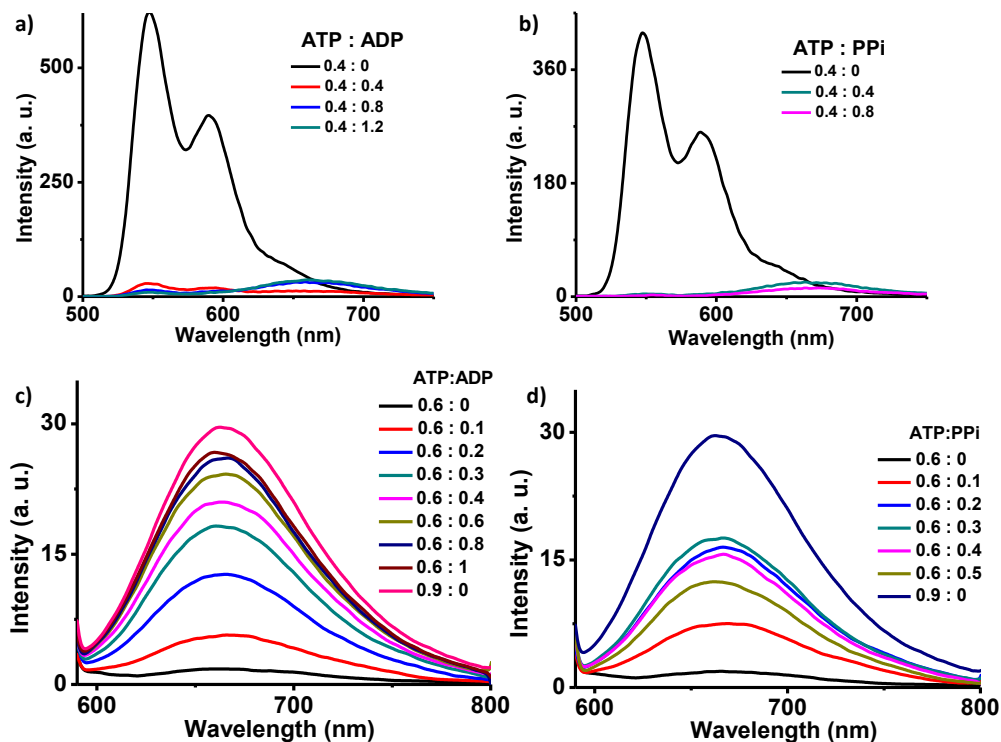


**Fig. S8** Variation in fluorescence spectra upon binding of a) ADP and b) PPI to the **H1**-state of the PDPA-assembly pre-bound with 0.4 eq. of ATP ( $\lambda_{exc}=470\text{nm}$ ), suggesting the formation of **H2**-states. This is more clear upon the selective excitation of the assembly at 570 nm, which is shown in c) and d) for ADP and PPI, respectively. These emission signals show heterotropic allosteric effect leading to transition from **H1** to **H2** state with PPI, ADP. (10 % MeCN in aq. HEPES solution,  $c = 2 \times 10^{-5}$  M).

It should be noted that, in the ADP case the emission intensity reaches close to that of ATP alone (ATP:ADP = 0.9:0), whereas in PPI case only half the intensity could be achieved, again due to the competitive replacement of ATP by PPI.

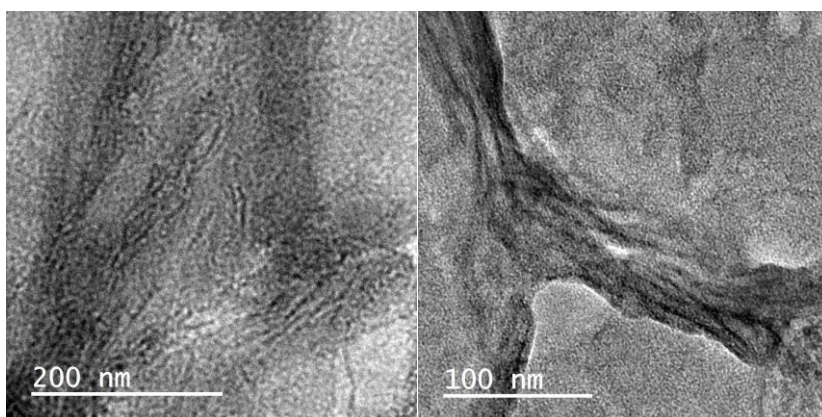


**Fig. S9** TEM images of nanofibers obtained upon addition of PPI to **H1**-state (0.25 eq. PPI + 0.5 eq. ATP, 10 % MeCN in water,  $c = 2 \times 10^{-5}$  M) through heterotropic allosteric regulation.

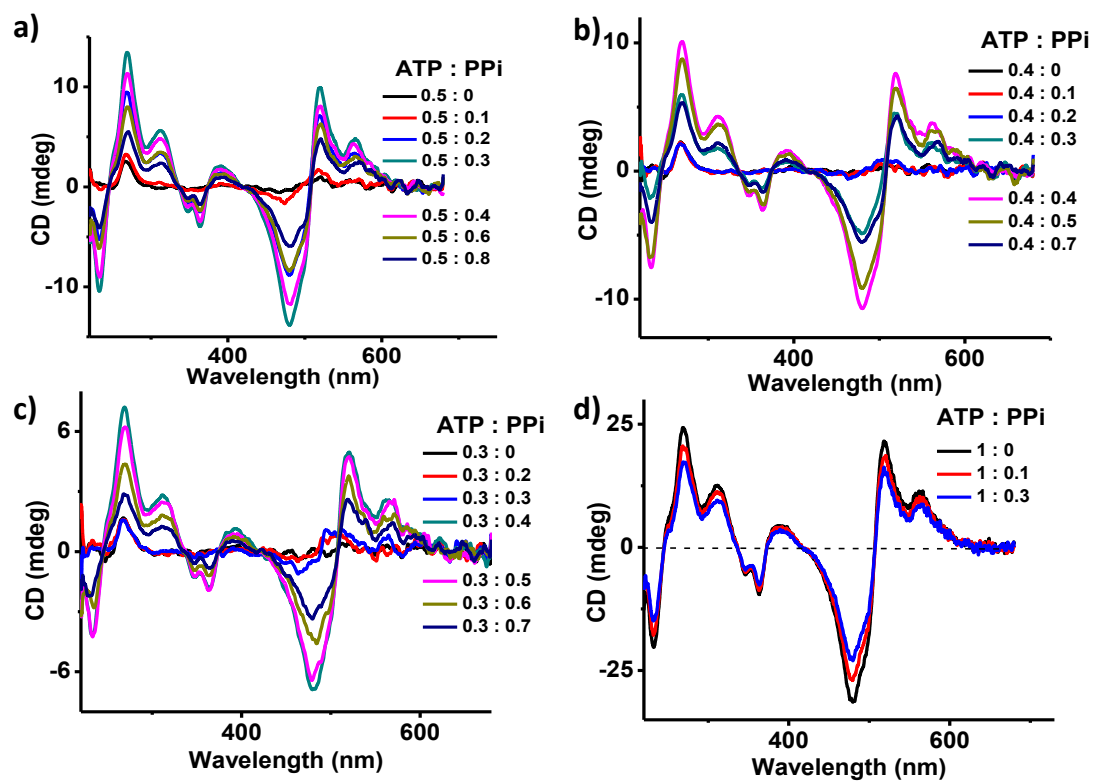


**Fig. S10** Evolution of CD signal upon addition of increasing eq. of PPI to **PDPA**-assembly pre-bound with a) 0.5 eq., b) 0.4 eq. c) 0.3 eq. and d) 1 eq. of ATP. (10 % MeCN in aq. HEPES solution,  $c = 2 \times 10^{-5}$  M). Higher amounts of PPI begin to decrease the CD intensity due to competitive replacement of ATP by PPI. These correspond to *Figure 4a* of the main text, where we see that higher equivalents of PPI tend to decrease the signal intensity. Legends in the graph represent molar equivalents of ATP with respect to **PDPA**.

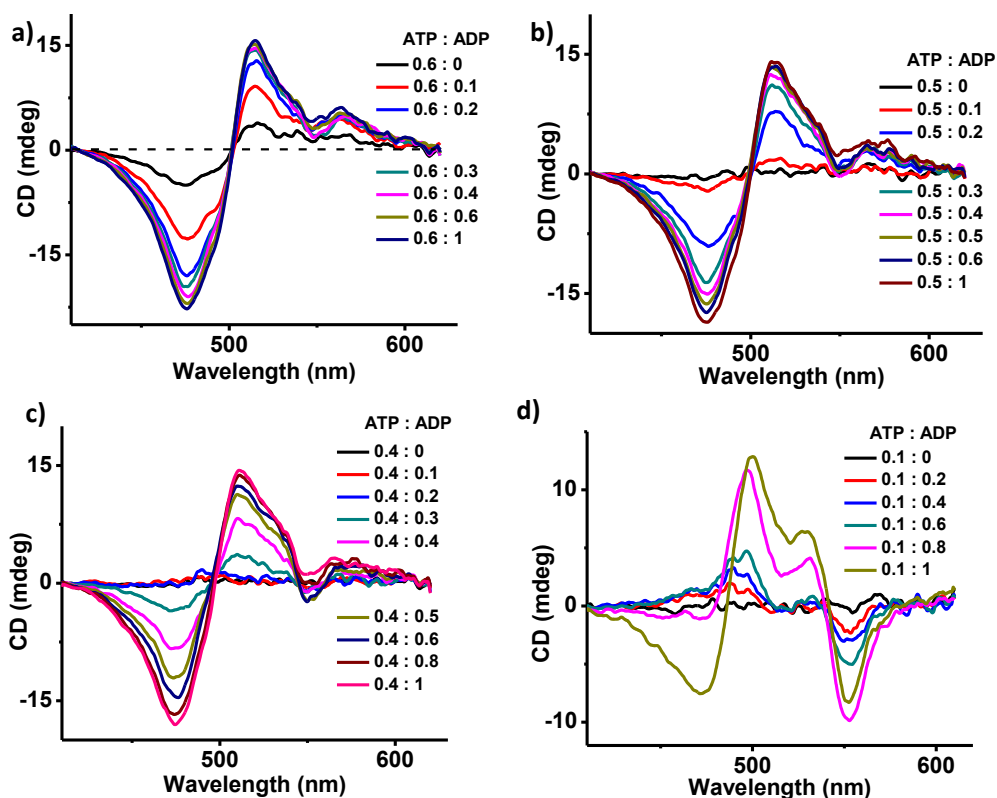


**Fig. S11** Evolution of CD signal upon addition of increasing eq. of ADP to **PDPA**-assembly pre-bound with a) 0.6 eq., b) 0.5 eq., c) 0.4 eq. and d) 0.1 eq. of ATP. (10 % MeCN in aq. HEPES solution,  $c = 2 \times 10^{-5}$  M). Legends in the graph represent molar equivalents with respect to **PDPA**.

At 0.1 eq. ATP in Figure S10d we observe that initial addition of ADP shows signal corresponding to ADP bound stacks which is opposite in direction to the **H2**-state. Further ADP addition leads to manifestation of **H2**-state, thereby co-existence of two bisignated signals i.e. one from only ADP bound portion and other from ATP bound **H2**-state. Due to non-enantiomeric nature of these ATP and ADP bound stacks which are not exactly mirror images, their co-existence in a given solution could be easily visualized in CD signal. Such observations confirm the fact that parts of the stacks which are free from ATP do not undergo allosteric regulation and they behave independently.

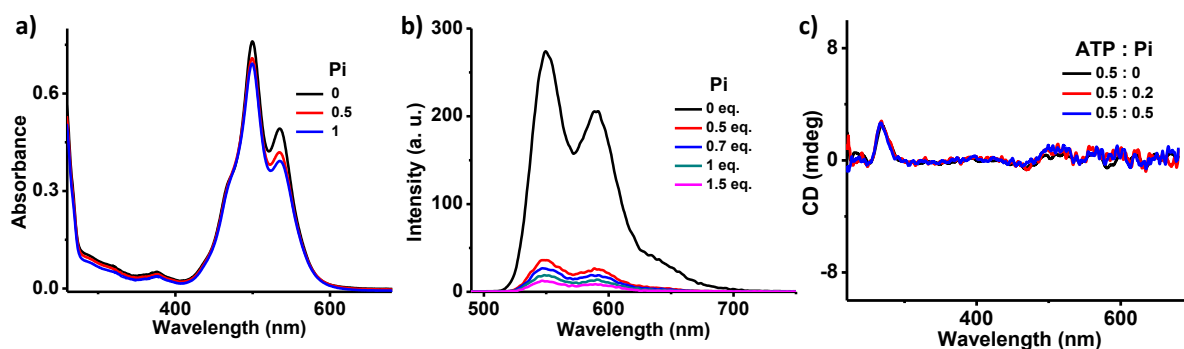


**Fig. S12** Variation in a) absorption spectra, b) emission spectra of **PDPA**-assembly on titration with Pi. c) shows changes in the CD signal on addition of Pi to **H1**-state (0.5 eq. ATP). (10 % MeCN in aq. HEPES solution,  $c = 2 \times 10^{-5}$  M).

Whereas absorption and emission spectra shows that Pi also bind to **PDPA** stacks, but fails to convert into **H2** state, even in presence of 0.5 eq. ATP.

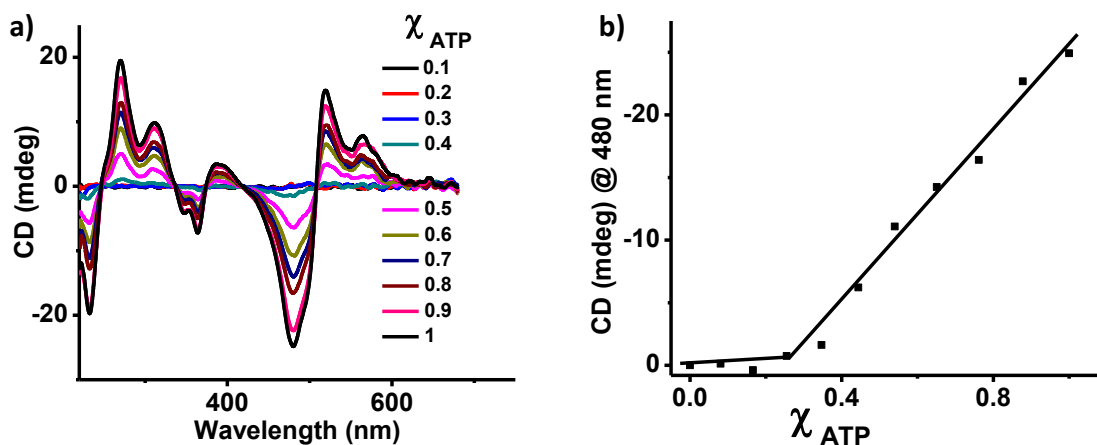


**Fig. S13** Sergeant and soldiers like experiment of the H2-state of the PDPA-assembly performed with a mixture of ATP and PPI. a) CD signal with varying molar ratios of ATP-PPI b) shows respective plot of CD intensity against mole fraction of ATP monitored at 480 nm. (10 % MeCN in aq. HEPES solution,  $c = 2 \times 10^{-5}$  M). Legends in the graph represent molar equivalents with respect to PDPA concentration.

The initial lag in c) till  $\chi_{ATP} = 0.3$  (i.e. 0.25 eq.) is due to the allosteric effect of ATP where initial equivalents of ATP do not show any CD signal. However, the linear response in CD signal clearly suggests the absence of chiral amplification in the present system.

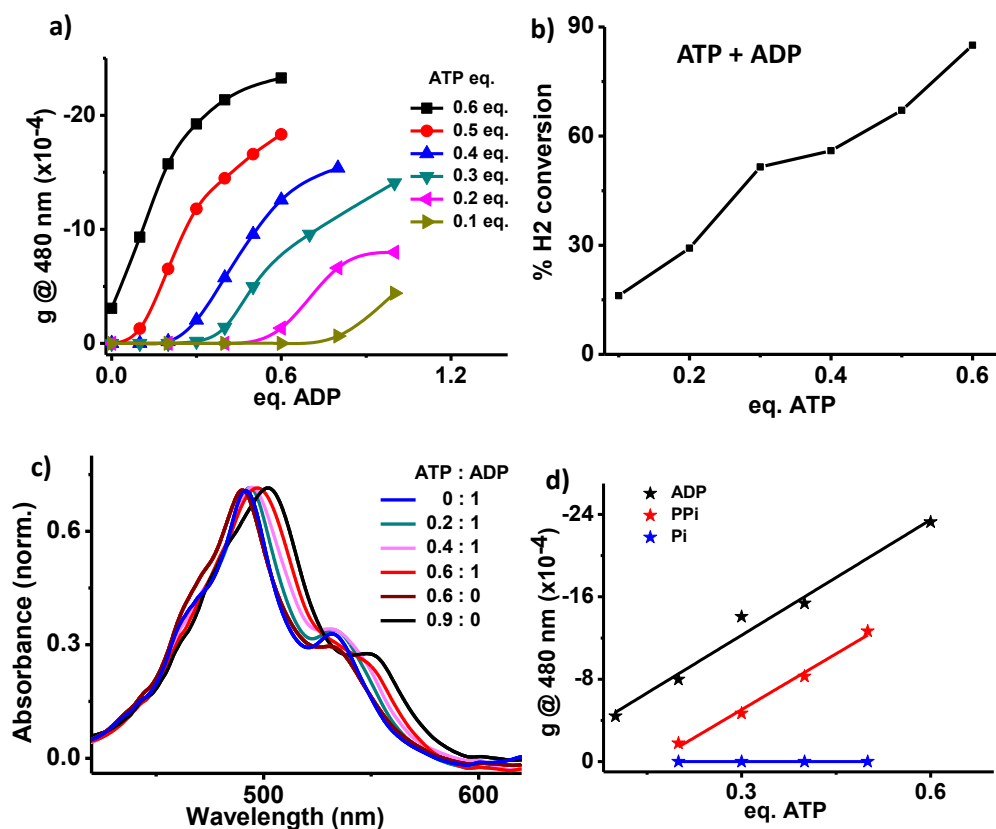


**Fig. S14** a) Shows plot of anisotropy value or g-value on ADP titration with varying eq. of ATP, whereas b) shows the percentage H2-conversion upon addition of ADP to H1-state (calculated with respect to g-value of ATP bound H2 with  $g_{ATP(max)} = 27.3 \times 10^{-4}$ ). c) Change in the absorption spectra upon addition of 1 eq. ADP to H1-states created with varying eq. of ATP. d) Plot of ascending eq. of pre-bound ATP versus the maximum anisotropy value or g-value attained for the H2-states with different heterotropic guests, which show a positive slope with PPI and ADP.

As seen in a), amount of ADP required for the CD signal to start rising goes on increasing with decreasing eq. of ATP. This is in line with the explanation that initially only one side of the chromophores bind to phosphates before second side binding starts. Same explanation holds good for Figure 4a.

In c) we see that at 0.6 eq. ATP, addition of ADP indeed leads of red shifted absorption expected of H2 state, but with lower absorbance. This is due to the inherent weaker association of ADP compared to ATP, which might affect the interchromophoric interactions leading to slightly lower effects. This is also supported by only 83 % recovery of **H2**-state, when compared with the **H2** obtained from ATP alone as shown in b).

In d) we notice that the conversion to H2 state on PPI or ADP binding is not 100 %, which can be either due to inherent lower strength of ADP/PPI binding when compared to ATP and competitive replacement of ATP by ADP/PPI.

## Reference

S1 X. Chen, M. J. Jou, J. Yoon, *Org. Lett.* 2009, **11**, 2181.